Clinical Imaging 40 (2016) 745–750

Contents lists available at ScienceDirect

Clinical Imaging

journal homepage: http://www.clinicalimaging.org

Original Article

Visibility of prostate cancer on transrectal ultrasound during fusion with multiparametric magnetic resonance imaging for biopsy

Wendy J.M. van de Ven [a,*], J.P. Michiel Sedelaar [b], Marloes M.G. van der Leest [a], Christina A. Hulsbergen-van de Kaa [c], Jelle O. Barentsz [a], Jurgen J. Fütterer [a], Henkjan J. Huisman [a]

[a] Department of Radiology and Nuclear Medicine, Radboud University Medical Center, Nijmegen, The Netherlands
[b] Department of Urology, Radboud University Medical Center, Nijmegen, The Netherlands
[c] Department of Pathology, Radboud University Medical Center, Nijmegen, The Netherlands

ARTICLE INFO

Article history:
Received 5 November 2015
Received in revised form 13 January 2016
Accepted 3 February 2016

Keywords:
Lesion visibility
MR-US fusion
PIRADS
Prostate cancer
Ultrasonography

ABSTRACT

Objectives: To determine transrectal ultrasound (TRUS) visibility of magnetic resonance (MR) lesions.
Methods: Data from 34 patients with 56 MR lesions and prostatectomy were used. Five observers localized and determined TRUS visibility during retrospective fusion. Visibility was correlated to Prostate Imaging–Reporting and Data System (PIRADS) and Gleason scores.
Results: TRUS visibility occurred in 43% of all MR lesions and in 62% of PIRADS 5 lesions. Visible lesions had a significantly lower localization variability. On prostatectomy, 58% of the TRUS-visible lesions had a Gleason 4 or 5 component.
Conclusions: Almost half of the MR lesions were visible on TRUS. TRUS-visible lesions were more aggressive than TRUS-invisible lesions.

1. Introduction

Currently, the most commonly used method to diagnose prostate cancer is transrectal ultrasound (TRUS)-guided biopsy. Localization of malignant tissue on TRUS is, however, difficult because most lesions are not visible [1]. TRUS-guided biopsy is therefore at random and can miss or undersample aggressive tumors and detect indolent cancers by chance [2,3].

Multiparametric magnetic resonance (mp-MR) imaging has shown to be highly accurate in detecting and localizing intermediate and highly aggressive cancers [4–6]. Recently, a standardized Prostate Imaging–Reporting and Data System (PIRADS) to detect intermediate and high-grade cancers on mp-MR imaging was introduced [7], which showed to improve diagnostic accuracy [8,9].

Targeted magnetic resonance (MR)-image-guided biopsy techniques are a very promising alternative to systematic TRUS-guided biopsy. In this respect, many different techniques are rapidly emerging, including direct in-bore MR, computer-assisted MR-TRUS fusion, and cognitive MR-TRUS fusion guidance. All of these techniques use prebiopsy MR imaging to define potential lesions for targeted biopsy. However, not all of them are equally accurate [10].

The first technique is in-bore MR targeted biopsy, which has been shown to significantly increase the tumor detection rate compared to systematic TRUS-guided biopsy especially for the clinically significant tumors [11] and reduces TRUS undergrading of aggressive tumors [12]. The second and potentially more accessible and practical solution is computer-assisted MR-guided TRUS fusion biopsy [13]. Clinical studies show that targeted prostate biopsy using MR-TRUS fusion has an increased tumor detection rate especially for clinically significant tumors [14–22]. The third technique is cognitive targeting. Reported results are contradictory [14,17]. As the accuracy of cognitive fusion strongly depends on the skills of the operating physician, it is likely that this technique is only effective in the hands of a TRUS and an MR expert.

We noted that some MR-detected lesions are retrospectively visible on TRUS. These lesions may, therefore, be more accurately targeted on both computer-assisted and cognitive MR-TRUS fusion biopsies. These TRUS-visible lesions may even be successfully targeted solely on TRUS, thereby providing more representative biopsy cores. A recent study by Ukimura et al. [23] showed that TRUS visibility may indeed facilitate targeted biopsies. However, they did not look at the visibility of lesions on TRUS with prior knowledge of MR appearance and PIRADS score. They also did not investigate correlation with Gleason scores.

* Corresponding author. Department of Radiology and Nuclear Medicine, Radboud University Medical Center, PO Box 9101, 6500 HB, Nijmegen, The Netherlands. Tel.: +31-24-361-45-45; fax: +31-24-354-08-66.
E-mail address: Wendy.vandeVen@radboudumc.nl (W.J.M. van de Ven).

http://dx.doi.org/10.1016/j.clinimag.2016.02.005
0899-7071/

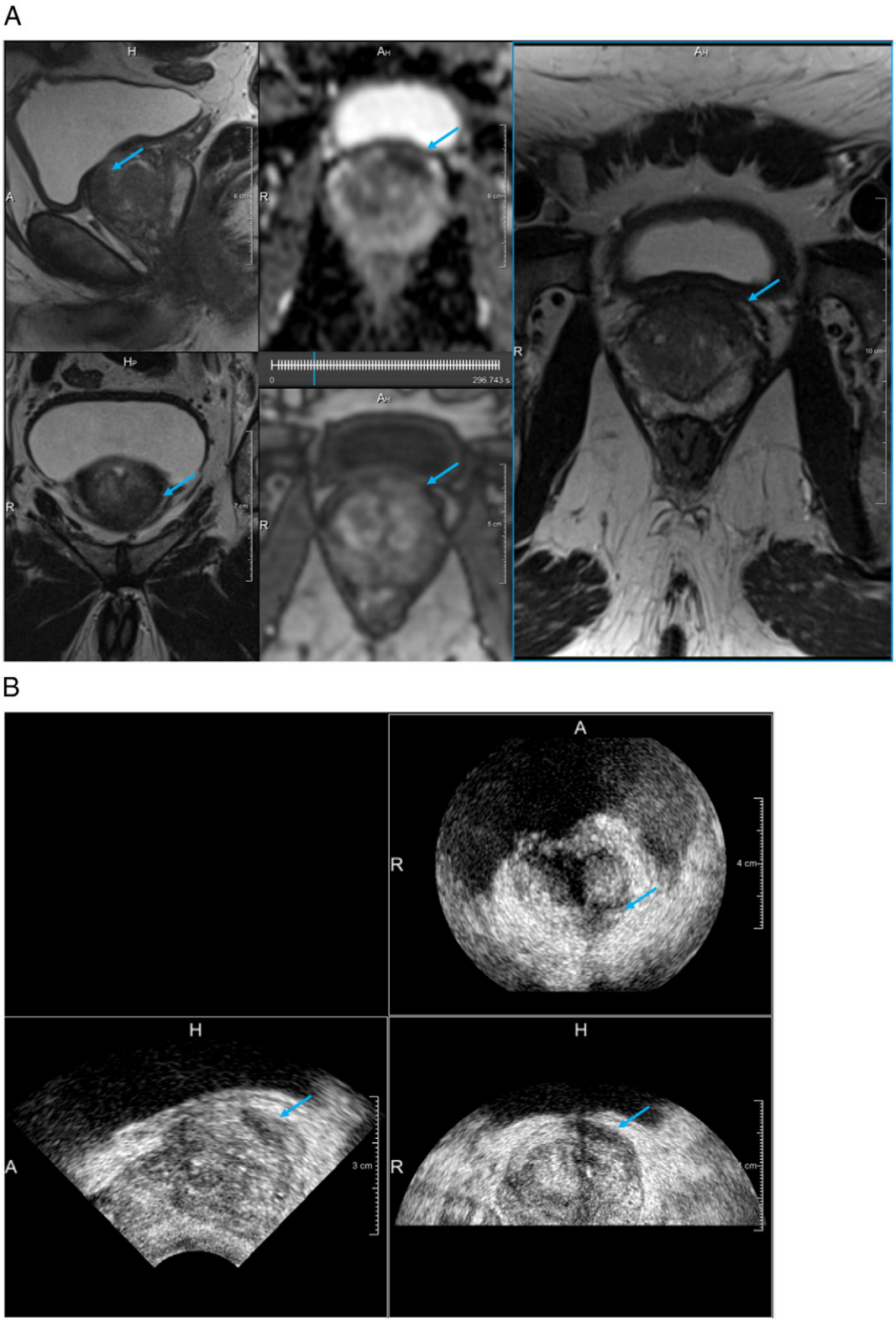

Fig. 1. (A) mp-MR images showing a PIRADS 5 lesion (indicated by the blue arrow). (B) Corresponding ultrasound image. Visibility score of the lesion was 5 for all observers.

Knowledge on correlation of TRUS visibility with PIRADS and Gleason scores will help to predict whether the lesion requires a biopsy and to predict if a lesion will be visible on TRUS images. Our study is a first step to gather knowledge on TRUS lesion visibility.

The aim of this retrospective observer study was to determine the proportion of MR suspicious lesions that are visible on TRUS.

2. Patients and methods

2.1. Patient selection

Data in this study were collected retrospectively from the data of the Radboudumc within the ongoing Prostate Cancer Molecular Medicine

Table 1
Summary of patient demographics

Parameter	Value
No. of patients	34
Median age (years)	63 (50–70)
Median PSA (ng/ml)	8.0 (2.5–30.0)
Median Gleason score	7 (4–9)
Clinical stage	
T2	22
T3	12

(PCMM) project. The PCMM project is a multicenter study focusing on prostate cancer detection. The inclusion criteria for the PCMM study were patients with localized prostate cancer confirmed by biopsy who were scheduled for radical prostatectomy in our institution. The institutional review board approved the study, and all patients gave their written informed consent.

Between December 2010 and August 2013, 48 consecutive PCMM patients diagnosed with prostate cancer at our center were included. Fourteen patients did not have a TRUS or prostatectomy. In the remaining 34 patients, a total of 56 lesions were prospectively detected on mp-MR imaging. For those 56 lesions, prostatectomy results were available.

2.2. MR imaging

In all patients, mp-MR imaging was performed according to the European Society of Urogenital Radiology guidelines [7] using a 3-T MR scanner (MAGNETOM Trio or Skyra; Siemens, Erlangen, Germany) either with a pelvic phased-array coil or a combination of an endorectal and pelvic phased-array coil.

The mp-MR imaging protocol included anatomical T2-weighted images in axial, coronal, and sagittal planes. Axial diffusion-weighted imaging (DWI) was acquired and apparent diffusion coefficient maps were automatically calculated. Dynamic contrast-enhanced MR images were obtained using a gadolinium-based contrast agent.

One expert radiologist with 20 years of experience in prostate MR image interpretation evaluated the images, using structured PIRADS reporting [7,24,25]. To assess the final score, a "dominant sequence weighting" was used, being DWI for peripheral zone and T2-weighted imaging for transition zone.

2.3. TRUS imaging

The PCMM project involved collecting TRUS images for study purposes. TRUS images were collected after MR imaging and the performing physician was aware of the MR results. The TRUS images were acquired on a Toshiba Aplio XG/Aplio 500 machine (Toshiba Medical Systems, Japan) using a four-dimensional end-firing transrectal transducer (Toshiba PVT-681MV; Toshiba Medical Systems, Japan) containing an internal, automatically tiltable convex element producing wedge-shaped three-dimensional (3D) volumes. The 3D grayscale TRUS images of the prostate were acquired with a scanning angle of 70°/90° and an acquisition rate of 0.1/0.2 volumes per second. The 3D raw image data were exported from the US machine and converted from a polar into a Cartesian representation with an isotropic voxel size of 0.2 mm.

Table 2
Distribution of PIRADS scores for MR lesions and visibility per PIRADS score

PIRADS	Amount	Number visible	Visibility (95% CI)
1	0	0	–
2	11	1	9.1% (1.6–37.7%)
3	3	0	0.0% (0.0–56.2%)
4	8	2	25.0% (7.2–59.1%)
5	34	21	61.8% (45.0–76.1%)
Index lesion	34	19	55.9% (39.5–71.1%)
All	56	24	42.9% (30.1–55.9%)

2.4. Histopathology

After radical prostatectomy, prostate specimens were uniformly processed and entirely submitted for histological investigations. After histological staining, all specimens were evaluated by one of two expert urological pathologists, one with 20 years of experience and one with 8 years of experience. The entire tumor volume was outlined on each step section. Each individual tumor was graded according to the 2005 International Society of Urological Pathology Modified Gleason Grading System [26] and staged according to the 2002 TNM classification.

2.5. Observer experiment

The anonymized mp-MR images and grayscale TRUS images were shown retrospectively in identical order to five observers, who analyzed the images independently. The PIRADS scores of all MR lesions were visible. Observers were aware that patients were scheduled for radical prostatectomy, but they did not have knowledge of the pathology outcomes. The observers varied in expertise: two observers were researchers with experience in prostate image analysis and MR-TRUS fusion biopsies, one observer was a urologist performing MR-TRUS fusion biopsies, and two observers were radiologists experienced in prostate MR imaging (one performing MR-TRUS fusion biopsies and the other radiologist had no experience in prostate ultrasound).

All observers were asked to determine the visibility of prostate lesions on prerecorded 3D TRUS images using an interactive in-house developed tool installed on a desktop in a lit office. Each of them had to perform cognitive fusion of MR and TRUS images. Three orthogonal views of the TRUS images were presented, and the observers had the possibility to translate and rotate the TRUS images around the three axes to allow cognitive fusion. Scrolling, zooming, and window leveling could be adjusted manually to optimize visibility.

The observers were asked to mark the center of the location of all 56 lesions on TRUS (example shown in Fig. 1). All readers assigned a 5-point visibility score to each of the lesions (1: definitely not visible; 2: probably not visible; 3: uncertain; 4: probably visible; 5: definitely visible). If the prostate could not be fully displayed due to restrictions of the TRUS probe, the observer could pick a sixth option "out of view".

2.6. Data analysis

Statistical proportion analysis was performed to determine the amount of lesions visible, subdivided into PIRADS score and index lesions (i.e., most aggressive lesions) only.

The proportion of visible lesions for different PIRADS assessments was determined including the 95% confidence intervals. A lesion was considered visible if at least three of the five observers scored a 4 or a 5 on the 5-point visibility scale.

The observer variability of the tumor location on TRUS was determined by calculating the distance to the mean location as pointed out by the observers. A small distance is likely to be an indication for a good localization of the lesion on TRUS during biopsy.

The averaged localization distances are grouped according to PIRADS and visibility score. An analysis of variance (ANOVA) is performed to determine significance.

Each MR lesion was correlated to the pathology outcomes by means of visual inspection of the corresponding prostatectomy specimen and Gleason scores were noted. The pathology outcomes were grouped by visibility of the lesion on TRUS images to investigate whether TRUS visibility correlates with Gleason score.

Differences were considered to be significant when $P<.05$. Statistical analyses were performed with Matlab (version 7.14.0; The Mathworks, Inc., Natick, MA).

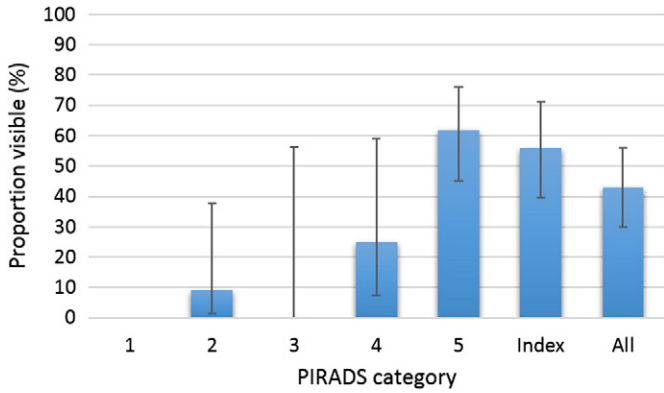

Fig. 2. Tumor visibility on TRUS according to PIRADS score, with additional categories for index and all lesions. Proportion (%) including 95% confidence intervals is shown as error bars.

3. Results

MR and TRUS images were collected in 34 patients. They had a median age of 63 years and a median PSA of 8.0 ng/ml (Table 1). In total, 56 lesions were detected on the mp-MR images. PIRADS 5 was present in 61%, PIRADS 4 was present in 14%, PIRADS 3 was present in 5%, and PIRADS 2 was present in 20% (Table 2). Of the PIRADS 2 lesions, 55% was not the most suspicious (index) lesion.

Of all lesions, 43% (24/56) were assessed as visible (score of 4 or 5) on TRUS by at least three observers. When only index lesions were taken into account, 56% (19/34) were visible. Of the PIRADS 4 and 5 lesions, 55% (23/42) were visible on TRUS. For PIRADS 5 lesions, this was 62% (21/34). One of the PIRADS 4 lesions was "out of view" according to four of the five observers, and therefore, it was also considered "invisible". The results and 95% confidence intervals are provided in Table 2 and Fig. 2.

The MR-detected lesions were predominantly located in the peripheral zone (47/56). Of these lesions, 47% (22/47) were visible on TRUS. Of the remaining nine transition zone lesions, two (22%) were visible on TRUS.

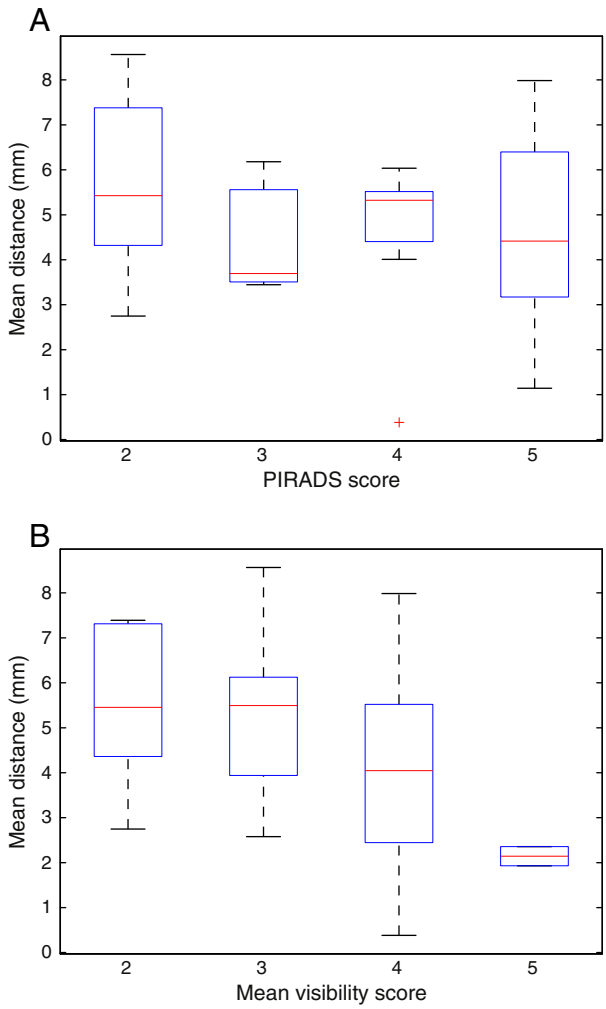

Fig. 3. Mean distances of the tumor location on ultrasound grouped according to (A) PIRADS classification and (B) mean visibility score.

Table 3
Distribution of Gleason scores (GS) grouped according to the visibility of the tumor on TRUS

	Negative	GS 4	GS 5	GS 6	GS 7		GS 8	GS 9
					3+4	4+3		
Visible	2	0	2	6	7	5	0	2
Invisible	12	1	4	4	4	3	2	2
Total	14	1	6	10	11	8	2	4

The overall localization variability of lesions, expressed as the distance to the mean location, on TRUS varied from 0.4 to 18.7 mm (mean 4.9 ± 3.2 mm); when averaged between the observers, the range was 0.4–8.6 mm. Larger distances corresponded to a lesion considered not visible by one or more observers; the localization variability for the visible lesions was 2.1 mm. Boxplots showing the averaged distances per lesion grouped according to their PIRADS classification and mean visibility score are shown in Fig. 3. Visibility score shows a strong correlation with the distance, i.e., visible lesions have a lower variability. An ANOVA showed a significant difference ($P = .016$) for the localization variability grouped according to mean visibility score, but not for PIRADS classification ($P = .378$).

The distribution of Gleason scores for visible and invisible lesions is shown in Table 3 and summarized in Fig. 4. Of the TRUS-visible lesions, 58% (14/24) were Gleason 7 or higher on prostatectomy and 83% (20/24) had a Gleason 6 or higher (see Fig. 4). Of the lesions that were not visible on TRUS, this was 34% (11/32) and 47% (15/32), respectively. Of the TRUS-invisible lesions, 38% (12/32) were negative on prostatectomy specimen; for the visible lesions, this was only 8% (2/24).

4. Discussion

In our study, we found that 43% of the MR-detected lesions were considered visible on TRUS. In PIRADS 4 and 5 lesions, this was the case in 55%. For the PIRADS 5 lesions, the TRUS visibility increased to 62%. Thus, more than half of the potential biopsy targets can be visible on TRUS when using the information from mp-MR imaging. For these cases and especially the PIRADS 5 cases, any targeted TRUS-guided biopsy method will benefit from TRUS lesion visibility, increasing the chance of obtaining a representative biopsy.

To our knowledge, our study is the first to investigate the visibility of prostate lesions on TRUS with prior knowledge of mp-MR images. There are publications on the incidence of hypoechoic, hyperechoic, and isoechoic lesions in TRUS-guided biopsies and also on targeted biopsies based on ultrasound appearance [27–30]. Hypoechoic areas have a 17–57% chance of being cancer [1]. Targeting all hypoechoic nodules will therefore result in a relatively low cancer detection rate; thus, it is important to know which are suspicious. Our results show that it may be possible to use prior knowledge of mp-MR imaging for selecting the hypoechoic lesions that require biopsy while indicating other hypoechoic areas that may be ignored. However, further research is required to determine if this is indeed possible. Also, more radiologists with different levels of expertise should then be included to investigate how this affects the results.

The location of the tumor on TRUS was well reproducible between observers. When averaged between observers, distances to the mean location per lesion varied between 0.4 and 8.6 mm. Most of the distances were well below the clinically significant tumor size (diameter of 10 mm). Larger distances were seen if an observer scored a 1 or a 2 for visibility on TRUS. The observers agreed significantly better on the location of the visible lesions. The visible lesions may thus be accurately targeted with MR-TRUS fusion biopsy.

More than half of the TRUS-visible tumors corresponded to Gleason 7 or higher, indicating that these contain a Gleason 4 or 5 component. Only one third of the invisible lesions had Gleason 7 or higher, and the remaining one third was negative on prostatectomy. Therefore, we can conclude that intermediate- and high-grade prostate cancer is better visible on TRUS images compared to low-grade prostate cancer. Our data included two Gleason 8 lesions, which were not visible on TRUS. A potential explanation for this TRUS invisibility might be that both lesions were Gleason 3 + 5 = 8. Also, one of them was not suspicious on mp-MR imaging (PIRADS 2), and the other one was scored as PIRADS 5.

The ability to predict the TRUS visibility from MR suspiciousness would allow these lesions to be targeted with regular TRUS devices without fusion or would enhance the accuracy of cognitive or computer-assisted fusion systems. The visible lesions may be targeted under (direct) TRUS guidance and thus are less dependent on the registration accuracy. For the lesions that are not visible on TRUS, one can consider an in-bore MR-guided biopsy or a computer-assisted MR-TRUS fusion system (depending on the size of the lesion [31]).

Our results are in line with a recent study where fusion biopsy is investigated including TRUS suspicion [23]. In that study, it was shown that TRUS visibility facilitates targeted biopsies leading to a higher detection rate of significant cancer compared to systematic TRUS-guided biopsies. MR and TRUS images were assessed independently from each other and cancer suspiciousness was determined on a 3-point scale. MR suspicion correlated with TRUS suspicion and combining both will help to select the most suspicious lesions. Ukimura et al. did not look at the distribution among Gleason scores, for which we show that TRUS-visible lesions are also more aggressive than TRUS-invisible lesions.

A limitation of our study is that it has a selection bias; the data only contain patients who are scheduled for a prostatectomy. This thus does not represent the patient population with elevated PSA referred to detect their significant cancer. We can therefore not draw a conclusion on overall US visibility for a regular clinical biopsy cohort, which may

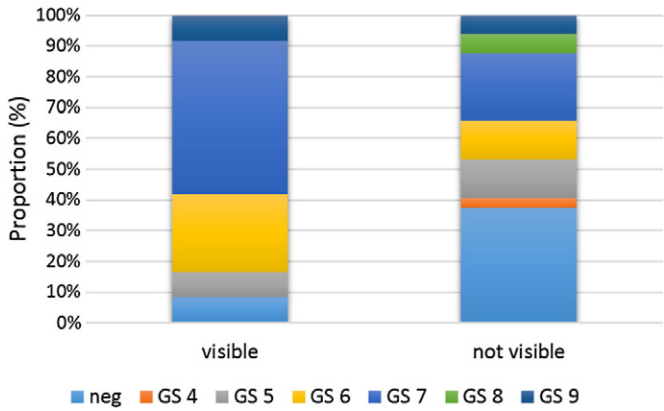

Fig. 4. Distribution of the pathology outcomes for lesions that were visible and not visible on TRUS images.

include smaller, lower-grade tumors and benign conditions. The number of lesions visible on TRUS may in this population be slightly lower. Also, the observers were aware of patients being scheduled for prostatectomy and had knowledge of the PIRADS scores. Another limitation is the small number of patients; thus, this study needs to be confirmed by other studies with higher number of patients. Nonetheless, the results are promising and significant.

The observers were provided with prerecorded 3D TRUS images. Although they were able to scroll through the prostate volume, they could not handle the probe themselves and assess "live" images. The TRUS images of the prostate often contain artifacts around urethra and bladder, which might be reduced when moving the probe during TRUS examination. In some cases, a lesion might not be visible due to TRUS artifacts, especially if it is located in the anterior part of the prostate. A lesion that is not visible on the prerecorded images may be visualized better during "live" TRUS. The proportion of visible tumors might then slightly increase.

In conclusion, we have shown that more than half of the lesions detected on mp-MR imaging were visible on TRUS; for PIRADS 5, this was almost two thirds. TRUS lesion visibility may help to improve finding the correct target location during MR-guided TRUS biopsy (both cognitive and computational fusions). Also, TRUS-visible lesions appeared to be more aggressive than invisible lesions; more than half of the visible lesions contain a Gleason 4 component or higher.

Acknowledgments

This work was funded by Grant No. KUN 2007-3971 of the Dutch Cancer Society.

References

[1] Heijmink SWTPJ, van Moerkerk H, Kiemeney LALM, Witjes JA, Frauscher F, Barentsz JO. A comparison of the diagnostic performance of systematic versus ultrasound-guided biopsies of prostate cancer. Eur Radiol 2006;16:927–38 [Available from: http://dx.doi.org/10.1007/s00330-005-0035-y].
[2] Norberg M, Egevad L, Holmberg L, Sparén P, Norlén BJ, Busch C. The sextant protocol for ultrasound-guided core biopsies of the prostate underestimates the presence of cancer. Urology 1997;50:562–6 [Available from: http://dx.doi.org/10.1016/S0090-4295(97)00306–3].
[3] Terris MK. Sensitivity and specificity of sextant biopsies in the detection of prostate cancer: preliminary report. Urology 1999;54:486–9.
[4] Fütterer JJ, Heijmink SWTPJ, Scheenen TWJ, Veltman J, Huisman HJ, Vos P, et al. Prostate cancer localization with dynamic contrast-enhanced MR imaging and proton MR spectroscopic imaging. Radiology 2006;241:449–58 [Available from: http://dx.doi.org/10.1148/radiol.2412051866].
[5] Kitajima K, Kaji Y, Fukabori Y, Yoshida K, Suganuma N, Sugimura K. Prostate cancer detection with 3 T MRI: comparison of diffusion-weighted imaging and dynamic contrast-enhanced MRI in combination with T2-weighted imaging. J Magn Reson Imaging 2010;31:625–31 [Available from: http://dx.doi.org/10.1002/jmri.22075].
[6] Tanimoto A, Nakashima J, Kohno H, Shinmoto H, Kuribayashi S. Prostate cancer screening: the clinical value of diffusion-weighted imaging and dynamic MR imaging in combination with T2-weighted imaging. J Magn Reson Imaging 2007;25:146–52 Available from: http://dx.doi.org/10.1002/jmri.20793.
[7] Barentsz JO, Richenberg J, Clements R, Choyke P, Verma S, Villeirs G, et al. ESUR Prostate MR Guidelines 2012. Eur Radiol 2012;22:746–57.
[8] Roethke MC, Kuru TH, Schultze S, Tichy D, Kopp-Schneider A, Fenchel M, et al. Evaluation of the ESUR PI-RADS scoring system for multiparametric MRI of the prostate with targeted MR/TRUS fusion-guided biopsy at 3.0 Tesla. Eur Radiol 2014;24:344–52 [Available from: http://dx.doi.org/10.1007/s00330-013-3017-5].
[9] Rosenkrantz AB, Kim S, Lim RP, Hindman N, Deng FM, Babb JS, et al. Prostate cancer localization using multiparametric MR imaging: comparison of prostate imaging reporting and data system (PI-RADS) and Likert scales. Radiology 2013;269:482–92 [Available from: http://dx.doi.org/10.1148/radiol.13122233].
[10] Moore CM, Robertson NL, Arsanious N, Middleton T, Villers A, Klotz L, et al. Image-guided prostate biopsy using magnetic resonance imaging-derived targets: a systematic review. Eur Urol 2013;63:125–40 [Available from: http://dx.doi.org/10.1016/j.eururo.2012.06.004].
[11] Hambrock T, Somford DM, Hoeks C, Bouwense SAW, Huisman H, Yakar D, et al. Magnetic resonance imaging guided prostate biopsy in men with repeat negative biopsies and increased prostate specific antigen. J Urol 2010;183:520–7 [Available from: http://dx.doi.org/10.1016/j.juro.2009.10.022].
[12] Hambrock T, Hoeks C, Hulsbergen-van de Kaa C, Scheenen T, Fütterer J, Bouwense S, et al. Prospective assessment of prostate cancer aggressiveness using 3-T diffusion-weighted magnetic resonance imaging-guided biopsies versus a systematic 10-core transrectal ultrasound prostate biopsy cohort. Eur Urol 2012;61:177–84 [Available from: http://dx.doi.org/10.1016/j.eururo.2011.08.042].
[13] Cornud F, Brolis L, Delongchamps NB, Portalez D, Malavaud B, Renard-Penna R, et al. TRUS-MRI image registration: a paradigm shift in the diagnosis of significant prostate cancer. Abdom Imaging 2013;38:1447–63 [Available from: http://dx.doi.org/10.1007/s00261-013-0018-4].
[14] Delongchamps NB, Peyromaure M, Schull A, Beuvon F, Bouazza N, Flam T, et al. Prebiopsy magnetic resonance imaging and prostate cancer detection: comparison of random and targeted biopsies. J Urol 2013;189:493–9 [Available from: http://dx.doi.org/10.1016/j.juro.2012.08.195].
[15] Hadaschik BA, Kuru TH, Tulea C, Rieker P, Popeneciu IV, Simpfendörfer T, et al. A novel stereotactic prostate biopsy system integrating pre-interventional magnetic resonance imaging and live ultrasound fusion. J Urol 2011;186:2214–20 [Available from: http://dx.doi.org/10.1016/j.juro.2011.07.102].
[16] Miyagawa T, Ishikawa S, Kimura T, Suetomi T, Tsutsumi M, Irie T, et al. Real-time virtual sonography for navigation during targeted prostate biopsy using magnetic resonance imaging data. Int J Urol 2010;17:855–60 [Available from: http://dx.doi.org/10.1111/j.1442-2042.2010.02612.x].
[17] Puech P, Rouvière O, Renard-Penna R, Villers A, Devos P, Colombel M, et al. Prostate cancer diagnosis: multiparametric MR-targeted biopsy with cognitive and transrectal US-MR fusion guidance versus systematic biopsy—prospective multicenter study. Radiology 2013;268:461–9 [Available from: http://dx.doi.org/10.1148/radiol.13121501].
[18] Siddiqui MM, Rais-Bahrami S, Truong H, Stamatakis L, Vourganti S, Nix J, et al. Magnetic resonance imaging/ultrasound-fusion biopsy significantly upgrades prostate cancer versus systematic 12-core transrectal ultrasound biopsy. Eur Urol 2013;64:713–9 [Available from: http://dx.doi.org/10.1016/j.eururo.2013.05.059].
[19] Sonn GA, Chang E, Natarajan S, Margolis DJ, Macairan M, Lieu P, et al. Value of targeted prostate biopsy using magnetic resonance-ultrasound fusion in men with prior negative biopsy and elevated prostate-specific antigen. Eur Urol 2013;65:809–15 [Available from: http://dx.doi.org/10.1016/j.eururo.2013.03.025].
[20] Walton Diaz A, Hoang AN, Turkbey B, Hong CW, Truong H, Sterling T, et al. Can magnetic resonance-ultrasound fusion biopsy improve cancer detection in enlarged prostates? J Urol 2013;190:2020–5.
[21] Mozer P, Rouprêt M, Le Cossec C, Granger B, Comperat E, de Gorski A, et al. First round of targeted biopsies with magnetic resonance imaging/ultrasound-fusion images compared to conventional ultrasound-guided trans-rectal biopsies for the diagnosis of localised prostate cancer. Br J Urol Int 2015;115:50–7 [Available from: http://dx.doi.org/10.1111/bju.12690].
[22] Delongchamps NB, Lefèvre A, Bouazza N, Beuvon F, Legman P, Cornud F. Detection of significant prostate cancer with magnetic resonance targeted biopsies—should transrectal ultrasound-magnetic resonance imaging fusion guided biopsies alone be a standard of care? J Urol 2015;193:1198–204.
[23] Ukimura O, Marien A, Palmer S, Villers A, Aron M, de Castro Abreu AL, et al. Transrectal ultrasound visibility of prostate lesions identified by magnetic resonance imaging increases accuracy of image-fusion targeted biopsies. World J Urol 2015 [Available from: http://dx.doi.org/10.1007/s00345-015-1501-z].
[24] Weinreb JC, Barentsz JO, Choyke PL, Curnud F, Haider MA, Macura KJ, et al. PI-RADS PIRADS imaging—reporting and data system: 2015, version 2. Eur Urol 2016;69:16–40.
[25] Barentsz JO, Weinreb JC, Verma S, Thoeny HC, Tempany CM, Shtern F, et al. Synopsis of the PI-RADS v2 guidelines for multiparametric prostate magnetic resonance imaging and recommendations for use. Eur Urol 2016;69:41–9.
[26] Epstein JI, Allsbrook WC, Amin MB, Egevad LL. ISUP Grading Committee. The 2005 International Society of Urological Pathology (ISUP) consensus conference on Gleason grading of prostatic carcinoma. Am J Surg Pathol 2005;29:1228–42.
[27] Fleshner NE, O'Sullivan M, Premdass C, Fair WR. Clinical significance of small (less than 0.2 cm^3) hypoechoic lesions in men with normal digital rectal examinations and prostate-specific antigen levels less than 10 ng/mL. Urology 1999;53:356–8.
[28] Onur R, Littrup PJ, Pontes JE, Bianco FJ. Contemporary impact of transrectal ultrasound lesions for prostate cancer detection. J Urol 2004;172:512–4 [Available from: http://dx.doi.org/10.1097/01.ju.0000131621.61732.6b].
[29] Spajic B, Eupic H, Tomas D, Stimac G, Kruslin B, Kraus O. The incidence of hyperechoic prostate cancer in transrectal ultrasound-guided biopsy specimens. Urology 2007;70:734–7 [Available from: http://dx.doi.org/10.1016/j.urology.2007.06.1092].
[30] Sperandeo G, Sperandeo M, Morcaldi M, Caturelli E, Dimitri L, Camagna A. Transrectal ultrasonography for the early diagnosis of adenocarcinoma of the prostate: a new maneuver designed to improve the differentiation of malignant and benign lesions. J Urol 2003;169:607–10 [Available from: http://dx.doi.org/10.1097/01.ju.0000045640.71845.b8].
[31] van de Ven WJM, Hulsbergen-van de Kaa CA, Hambrock T, Barentsz JO, Huisman HJ. Simulated required accuracy of image registration tools for targeting high-grade cancer components with prostate biopsies. Eur Radiol 2013;23:1401–7 [Available from: http://dx.doi.org/10.1007/s00330-012-2701-1].